

Letters to the Editor

Synthesis of nanoporous carbon with pre-graphitic domains

Christopher L. Burket^a, Ramakrishnan Rajagopalan^{a,c}, Henry C. Foley^{a,b,c,*}^a Department of Chemical Engineering, The Pennsylvania State University, University Park, PA 16802, United States^b Department of Chemistry, The Pennsylvania State University, University Park, PA 16802, United States^c Materials Research Institute, The Pennsylvania State University, University Park, PA 16802, United States

Received 13 February 2007; accepted 21 June 2007

Available online 28 June 2007

Porous carbons with tunable porosity and electrical conductivity have received considerable attention due to their potential application as anodes in lithium ion batteries, electrocatalysts in fuel cells, and high surface area electrodes in electrical double layer capacitors [1,2]. High porosities and surface areas are critical to the performances of these materials. Significant porosity and surface area are easily created by activation of non-graphitizing carbon, yet the material lacks in conductivity [3–5]. Whereas graphitic carbon possesses high conductivity, it strongly resists activation by traditional methods [5]. Recently graphitic carbons with controlled pore sizes have been obtained by pyrolysis of graphitizing carbon precursors deposited in mesoporous silica templates [2,6,7]. However, the preparation of carbon with nanopores,¹ width less than 2 nm, is unattainable by this method, thus limiting its ultimate surface area, porosity, and performance. Graphitization of non-graphitizing carbon occurs in the presence of a variety of metals, but the product is contaminated with the catalyst [8–11]. Stress graphitization of pure carbon has been reported at temperatures in excess of 2000 °C [12,13]. Porosity is not preserved. Herein we describe the discovery of a new route to the synthesis of a pure nanoporous carbon containing pre-graphitic structures with both high surface area and high nano- and mesoporosity from the readily available polymer precursor polyfurfuryl alcohol.

Nanoporous carbon (NPC) is synthesized by pyrolysis of polymers, such as polyfurfuryl alcohol (PFA). Due to its strong resistance to transformation to graphite even when annealed at temperature above 2000 °C, it is classified as non-graphitizing, which was defined by Franklin [14]. This resistance is attributed to the presence of extensive cross-linking in the precursor, which creates kinetically frozen disorder through a chaotic misalignment of the graphenes in the carbon that result during pyrolysis [15–17]. Disorder in NPC gives rise to porosity and the majority of pores are narrowly distributed in the range from 0.4 to 0.5 nm width [16,18,19]. The pore volume and surface area of NPC can be further developed by simple activation with CO₂ [20,21]. We have found that the pre-graphitic ordering of PFA-derived NPC can be accomplished after CO₂ treatment at 900 °C, which generates activated NPC (a-NPC). The a-NPC provides an unexpected pathway to pre-graphitic carbon with nanoporosity by subsequent annealing at 2000 °C.

First, *p*-toluenesulfonic acid monohydrate (0.048 gm, Sigma–Aldrich) was dissolved in 5 ml of Triton X-100 (Sigma–Aldrich) by heating mildly. Then to this solution, 5 ml of furfuryl alcohol (99% Sigma–Aldrich) was added. The reaction mixture was stirred magnetically at 10 °C. After polymerization for 48 h the product was transferred to a quartz boat and pyrolyzed under flowing argon in a quartz tube furnace. The sample was heated at a rate of 10 °C min⁻¹ to 800 °C and held for 1 h. The carbon product was pure, without inorganic contaminants. It was ground and sieved to a particle size of < 38 μm. Activated NPC was prepared in a quartz tube furnace. 0.5 gm of carbon was heated to 900 °C over 1 h in flowing argon. After 1 h of soak time the gas was switched to CO₂ and soaked for an additional 3.5 h. The sample was cooled back to room temperature under argon. High temperature

* Corresponding author. Address: Department of Chemical Engineering, The Pennsylvania State University, University Park, PA 16802, United States. Fax: +1 814 865 5604.

E-mail address: hcf2@psu.edu (H.C. Foley).

¹ The width of a nanopore does not exceed 2 nm. The IUPAC term for a pore of this dimension is micropore.

treatment (HTT) was carried out in a Red Devil furnace (R.D. Webb Company, Natick, MA). The hot zone was evacuated to 10^{-3} mbar for 24 h prior to backfilling and annealing under flowing argon. A $25\text{ }^{\circ}\text{C min}^{-1}$ heating rate was employed with a 1 h soak at $2000\text{ }^{\circ}\text{C}$. Other than degassing prior to annealing, all synthesis steps were carried out at atmospheric pressure. A methyl chloride adsorption isotherm was used to calculate the pore volume and pore width of the carbons according to the Horvath-Kawazoe and the Kelvin models in the nano- and meso-pore regions respectively [22].

Fig. 1 displays the powder X-ray diffraction (XRD) pattern of NPC after pyrolysis of polyfurfuryl alcohol at $800\text{ }^{\circ}\text{C}$. The broad (002) peak of NPC800 is typical of amorphous carbon and is indicative of a high degree of disorder in the layers of graphenes. A shift of the line to $2\theta = 24.2^{\circ}$ for NPC800 from $2\theta = 26.5^{\circ}$ for graphite denotes an average d_{002} of $3.68\text{ }\text{\AA}$, versus $3.35\text{ }\text{\AA}$ found in highly crystalline graphite. An average L_c of $10\text{ }\text{\AA}$ is calculated with the aid of

the Scherrer equation. From the (10) line, L_a is $15\text{ }\text{\AA}$. A transmission electron microscope (TEM) image is shown in Fig. 2a. The microstructure of NPC800 is confirmed to be globally amorphous without long-range order. The total and differential pore volumes of the carbon were determined and are given in Fig. 3. NPC800 has a total pore volume of $0.22\text{ cm}^3\text{ g}^{-1}$, with $0.17\text{ cm}^3\text{ g}^{-1}$ of nanopores. Its apparent N_2 BET surface area is $317\text{ m}^2\text{ g}^{-1}$, with an associated error of $11\text{ m}^2\text{ g}^{-1}$.

The resistance to graphitization of NPC800 was examined by annealing at $2000\text{ }^{\circ}\text{C}$. The pore structure of NPC2000 is rendered completely inaccessible, as seen in Fig. 3, and the apparent surface area drops to $22\text{ m}^2\text{ g}^{-1}$, with an associated error of $11\text{ m}^2\text{ g}^{-1}$. Non-graphitizing behavior is evident in the XRD pattern. Although a shift of the (002) line towards 26.5° , coupled with reduced broadening, indicates increased order, the average d_{002} is $3.50\text{ }\text{\AA}$ and significant stacking of the graphenes has not occurred as the L_c is just $15\text{ }\text{\AA}$. L_a is $27\text{ }\text{\AA}$. The carbon

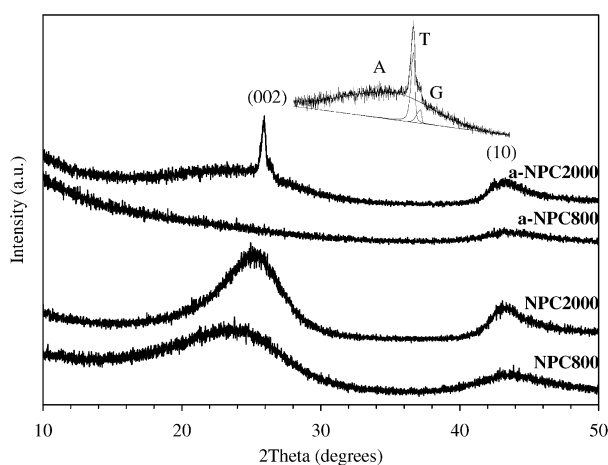


Fig. 1. Powder X-ray diffraction patterns of NPC as pyrolyzed at $800\text{ }^{\circ}\text{C}$ (NPC800), after annealing at $2000\text{ }^{\circ}\text{C}$ (NPC2000), after activation (a-NPC800), and after both activation and annealing (a-NPC2000). The inset shows the fit of the A-, T-, and G-components to the (002) peak.

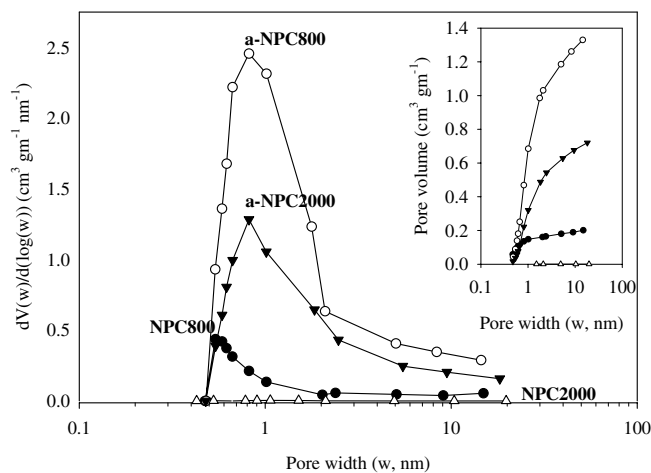


Fig. 3. Differential pore volume and total pore volume of NPC as pyrolyzed at $800\text{ }^{\circ}\text{C}$ (NPC800), after annealing at $2000\text{ }^{\circ}\text{C}$ (NPC2000), after activation (a-NPC800), and after both activation and annealing (a-NPC2000).

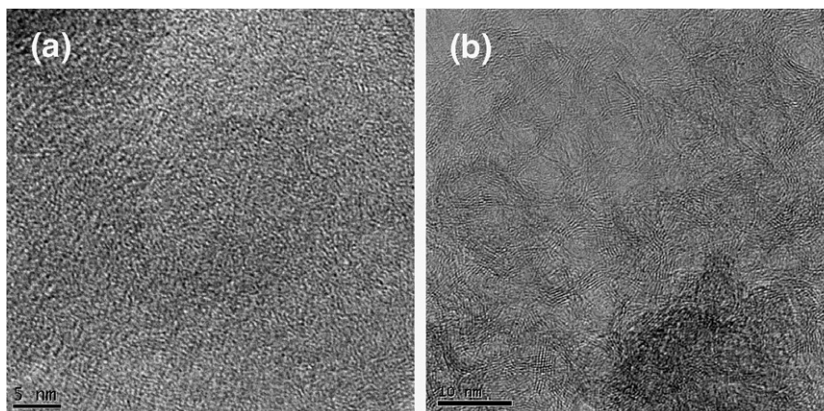


Fig. 2. TEM images of NPC (a) as pyrolyzed at $800\text{ }^{\circ}\text{C}$ and (b) annealed at $2000\text{ }^{\circ}\text{C}$.

remains globally amorphous. The TEM image of NPC2000 in Fig. 2b shows ribbons of stacked graphenes at most 10 layers thick. This structure is reminiscent of the classic non-graphitizing carbon model “Jenkin’s Nightmare”, where curved graphitic ribbons loop around each other with no preferred orientation in a three-dimensional network [5]. Further graphitization would require the rupture of strong carbon–carbon bonds within the entities making up the ribbons or at least the addition of sufficient thermal energy to allow for long range mobility and disentanglement.

Activation of NPC800 with CO₂ yields 18% by weight of a-NPC800, with an apparent surface area of 2135 m² g⁻¹ and a six fold increase in pore volume to 1.33 cm³ g⁻¹, see Fig. 3. The error on this surface area measurement is 52 m² g⁻¹. The nanopore width increases from 0.5 to a more accommodating 0.8 nm due to pore widening. Via X-ray photoelectron spectroscopy the atomic oxygen percentage was measured. The value decreases from 8.4% in NPC800 to 3.8% in a-NPC800. The (002) reflection is no longer present in the XRD pattern of a-NPC800 (Fig. 1). Intensity of the (002) line is due to stacking of graphenes in the domains which form the pore walls. Its absence indicates the pore wall thickness is reduced during activation. The TEM image in Fig. 4a depicts

an amorphous microstructure, although the density of graphenes is reduced, consistent with pore wall thinning during activation.

Annealing the activated carbon at 2000 °C for 1 h invokes a surprisingly dramatic increase in structural order of the carbon. A sharp (002) line is now observed at 26° in the powder XRD pattern of a-NPC2000 (Fig. 1). It is accompanied by a shoulder at 26.5°. The graphitic peaks of a-NPC2000 appear superimposed over a broader background peak, such as in NPC2000. The (002) line is resolved into three components: amorphous (A), turbostratic (T), and graphitic (G) [23,24]. The fit is shown in the Fig. 1 inset. Average layer spacings of the A, T, and G components are 3.66, 3.44, and 3.37 Å, respectively. The *L_c* of the A-component is just 10 Å, whereas the T- and G-components exhibit 276 and 145 Å domains. *L_a* is 27 Å. An abundance of microstructures are found in the TEM. Fig. 4b shows an ordered pre-graphitic structure, which corresponds to the T- and G-components, whereas Fig. 4c depicts the A-component. Fig. 4d demonstrates the intimate contact between the amorphous and pre-graphitic carbon. The pre-graphitic carbon contains graphenes stacked more than 20 layers thick. Unlike the non-activated sample, collapse of the pore structure is only partial in a-NPC2000, see Fig. 3. The retained pore volume is 0.72 cm³ g⁻¹, with 0.50 cm³ g⁻¹ distributed

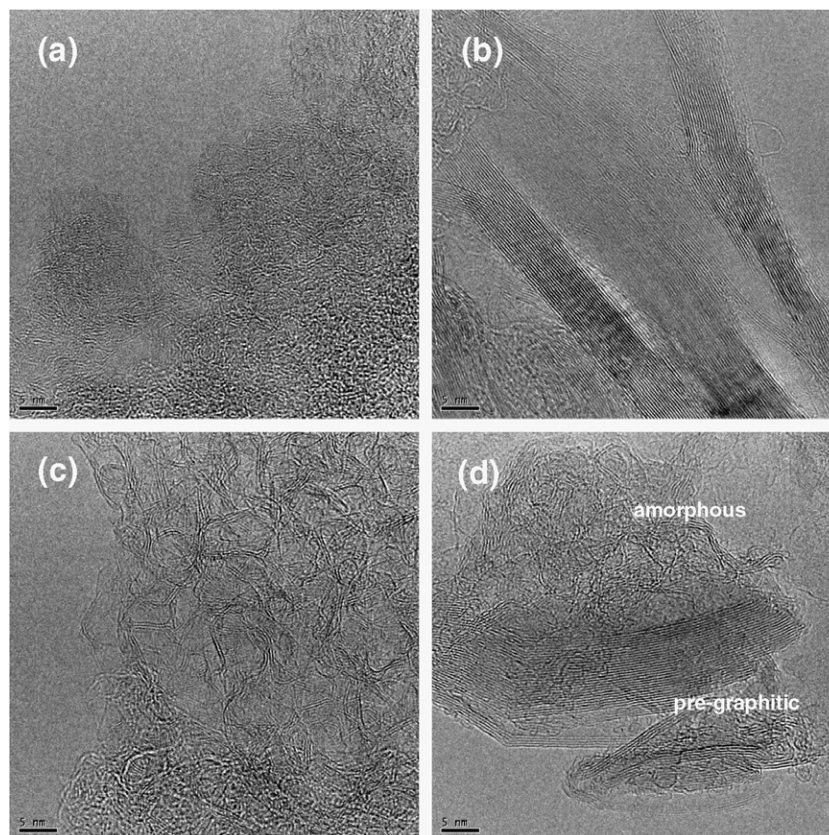


Fig. 4. TEM images of NPC (a) activated with CO₂ and (b,c,d) activated and annealed at 2000 °C. Pre-graphitic carbon (b) and amorphous carbon (c) are shown individually. Both amorphous and pre-graphitic carbons are also shown in intimate contact (d).

as nanopores and the other $0.22 \text{ cm}^3 \text{ g}^{-1}$ as mesopores. The pore width is preserved after annealing; it continues to be centered at 0.8 nm. An apparent surface area of $1060 \text{ m}^2 \text{ g}^{-1}$ also remains. The error associated with this surface area measurement is $52 \text{ m}^2 \text{ g}^{-1}$.

NPC pyrolyzed at $800 \text{ }^\circ\text{C}$ is non-graphitizing. The carbon is a disordered collection of graphenes, which are “kinetically frozen” and resistant to realigning to form long-range graphitic structures [16]. Although high temperature treatment at $2000 \text{ }^\circ\text{C}$ creates additional order in the material, it cannot be considered graphitic and the small degree of transformation that does occur under thermally forcing conditions occurs at the expense of complete collapse of the pore structure. Activation dramatically enhances the carbon porosity; an effect of which is a reduction in the number of graphenes in the pore wall. The thinner domains are more mobile and able to align themselves into both turbostratic and graphitic structures with long-range order when annealed at $2000 \text{ }^\circ\text{C}$. The structures are termed pre-graphitic as order extends in two dimensions. However, the conversion is incomplete and nanoporous amorphous carbon remains interspersed with the pre-graphitic structures. The inhomogeneous microstructure is advantageous. Molecular sieving nanopores with a width of 0.8 nm create surface area which can provide ready access to the crystallized regions.

In conclusion, this is a new pathway to synthesize nanoporous carbon with pre-graphitic domains; thinning the pore walls via activation reduces the barrier to graphitization. Subsequent high temperature treatment facilitates coalescence of the graphenes to form a pre-graphite structure which cannot be realized without activation.

Acknowledgement

Partial funding for this research was provided by NSF NIRT-DMR-0304391.

References

- [1] Lee J, Kim J, Hyeon T. Recent progress in the synthesis of porous carbon materials. *Adv Mater* 2006;18:2073–94.
- [2] Fuertes AB, Alvarez S. Graphitic mesoporous carbons synthesised through mesostructures silica templates. *Carbon* 2004;42:3049–55.
- [3] Frackowiak E, Beguin F. Carbon materials for the electrochemical storage of energy in capacitors. *Carbon* 2001;39:937–50.
- [4] Bleda-Martinez MJ, Macia-Agullo JA, Lozano-Castello D, Morallon E, Cazorla-Amoros D, Linares-Solano A. Lozano-Castello D, Morallon E, Cazorla-Amoros D, Linares-Solano A. Role of surface chemistry on electric double layer capacitance of carbon materials. *Carbon* 2005;42:2677–84.
- [5] Jenkins GM, Kawamura K. *Polymeric Carbons*. Cambridge: Cambridge University Press; 1976.
- [6] Kyotani T. Control of pore structure in carbon. *Carbon* 2000;38:269–86.
- [7] Fuertes AB, Centeno TA. Mesoporous carbons with graphitic structures fabricated by using porous silica materials as templates and iron-impregnated polypyrrole as precursor. *J Mater Chem* 2005;1079–83.
- [8] Jenkins RG, Walker PL. Small-angle X-ray-scattering studies on carbons derived from polyfurfuryl alcohol and polyfurfuryl alcohol-ferrocene copolymers. *Carbon* 1976;14(1):7–11.
- [9] Oya A, Mochizuki M, Otani S, Tomizuka I. Electron-microscopic study on the turbostratic carbon formed in phenolic resin carbon by catalytic action of finely dispersed nickel. *Carbon* 1979;17(1):71–6.
- [10] Oya A, Otani S. Catalytic graphitization of carbons by various metals. *Carbon* 1979;17(2):131–7.
- [11] Marsh H, Crawford D, Taylor DW. Catalytic graphitization by iron of isotropic carbon from polyfurfuryl alcohol, 725–1090 K – a high resolution electron-microscope study. *Carbon* 1983;21(1):81–87.
- [12] Franklin RE. Homogeneous and heterogeneous graphitization of carbon. *Nature* 1956;177(4501):239.
- [13] Honda H, Kobayash K, Sugawara S. X-ray characteristics of non-graphitizing-type carbon. *Carbon* 1968;6(4):517–23.
- [14] Franklin R. Crystallite growth in graphitizing and non-graphitizing carbons. *Proc Roy Soc* 1951;A209:196–218.
- [15] Fitzer E, Schafer W. The effect of crosslinking on the formation of glasslike carbons from thermosetting resins. *Carbon* 1970;8:353–64.
- [16] Mariwala RK, Foley HC. Evolution of ultramicroporous adsorptive structure in poly(furfuryl alcohol)-derived carbogenic molecular sieves. *Indus Eng Chem Eng* 1994;33:607–15.
- [17] Burket CL, Rajagopalan R, Marencic A, Dronavajjala K, Foley HC. Genesis of porosity in polyfurfuryl alcohol derived nanoporous carbon. *Carbon* 2006;44(14):2957–63.
- [18] Fitzer E, Schafer W, Yamada S. The formation of glasslike carbon by pyrolysis of polyfurfuryl alcohol and phenolic resin. *Carbon* 1969;7:643–8.
- [19] Foley HC. Carbogenic molecular sieves: synthesis, properties and applications. *Micropor Mater* 1995;4:407–33.
- [20] Rand B, Marsh H. The process of activation of carbons by gasification with CO_2 -III. Uniformity of gasification. *Carbon* 1971;9:79–85.
- [21] Marsh H, Rand B. The process of activation of carbons by gasification with CO_2 -I. Gasification of pure polyfurfuryl alcohol carbon. *Carbon* 1971;9:47–61.
- [22] Mariwala RK, Foley HC. Calculation of micropore sizes in carbogenic materials from the methyl chloride adsorption isotherm. *Indus Eng Chem Eng* 1994;33(10):2314–21.
- [23] Oya A, Marsh H. Review: phenomena of catalytic graphitization. *J Mater Sci* 1982;17:309–22.
- [24] Honda H, Kobayashi K, Sugawara S. X-ray characteristics of non-graphitizing-type carbon. *Carbon* 1967;6:517–23.